ELSEVIER

Journal of Alloys and Compounds 218 (1995) 157–164

Journal of ALLOYS AND COMPOUNDS

Room-temperature crystal structure of the layered phase $Cu^{I}In^{III}P_2S_6$

V. Maisonneuve, M. Evain, C. Payen*, V.B. Cajipe, P. Molinié

Institut des Matériaux de Nantes, Unité Mixte de Recherche associée au CNRS 0110, 2 rue de la Houssinière, 44072 Nantes Cedex 03, France

Received 2 February 1994; in final form 19 May 1994

Abstract

The room-temperature structure of $CuInP_2S_6$ was determined using single-crystal X-ray diffraction. It crystallizes in the monoclinic symmetry, space group *Cc*, with the lattice parameters $a=6.0956(4)$ Å, $b=10.5645(6)$ Å, $c=13.6230(8)$ Å, $\beta=107.101(3)°$, $V=838.5(1)$ Å^3 and $Z=4$. As for $CuCrP_2S_6$ and $CuVP_2S_6$, the layered structure consists of a succession of $(SCu^{I}_{1/3}In^{III}_{1/3}(P_2)_{1/3}S)$ slabs separated by empty van der Waals gaps. Within a slab, the octahedral voids defined by the ABC close-packed array of sulfur are filled by the metal cations and P_2 groups such that a triangular two-dimensional sublattice is formed by each of them. The Cu(I) ions are distributed on two inequivalent off-center sites with occupation ratios of about 0.9 and 0.1 per octahedron, and the In(III) ions are displaced from the center of their octahedra.

Keywords: Thiophosphate; Indium; Copper; X-Ray structure determination

1. Introduction

The two-dimensional (2D) MPS_3 phases, where M is a divalent transition metal (M≡Mn, Fe, Co, Ni, Zn or Cd), have been extensively studied because of their potential as cathodic materials as well as their interesting structural, chemical and physical properties [1–15]. These layered compounds are built from $(SM_{2/3}(P_2)_{1/3}S)$ slabs separated by empty van der Waals (vdW) gaps, with the M cations and P_2 groups occupying the octahedral sites of the close-packed array of sulfur anions so that a honeycomb metal network is formed [1]. Interest in these compounds has also been triggered by the many heterocharge metallic substitution possibilities that exist within this structural type. Indeed, substituted layered materials of types $M^{I}M'^{III}P_2S_6$ [16–21] and $M^{I}_{2x}M'^{II}_{2-x}P_2S_6$ [22–28] in which M(I)≡Ag or Cu, M′(II)=Mn, Cd or Zn and M′(III)=Sc, V, Cr or In have been prepared and characterized. The $M^{I}M'^{III}P_2S_6$ family has, in particular, stimulated investigations relevant to the questions of both transition metal ordering (coloring problem) [29] and one-dimensional antiferromagnetism [30,31].

More recent work has focused on the origin of the unusually extended shapes of the Ag(I) and Cu(I) electronic densities observed at room temperature (RT) in both types of MPS_3 substitution derivative. Most of the RT single-crystal refinements have used several "split" positions of incomplete occupancy to model these densities. In $CuCrP_2S_6$ for instance, the continuous copper electronic distribution perpendicular to the layers could be modeled by four positions inside the octahedra: two near the center and two close to two opposite triangular faces [16]. An additional pair of tetrahedral positions in the vdW gap was necessary for $CuVP_2S_6$ [21].

The fundamental problem of determining whether these smeared electronic densities represent a static or dynamic kind of disorder, or the coexistence of Cu_2S_6 entities and vacancies in the case of $CuM^{III}P_2S_6$ (M≡V or Cr), has motivated temperature-dependent structural studies [24,26,32–36]. In particular, low temperature neutron powder diffraction experiments on the $CuM^{III}P_2S_6$ compounds (M≡V or Cr) have been recently reported [34,35]. On the one hand, the 20 K pattern of the vanadium material revealed a repartitioning of Cu over only two sites (against six at RT) located within the sulfur triangles at the edge of the structure slabs, without any change of the crystal sym-

*Corresponding author.

0925-8388/95/$09.50 © 1995 Elsevier Science S.A. All rights reserved
SSDI 0925-8388(94)01416-7

metry (space group, $C2$) [34]. On the other hand, the copper ions in $CuCrP_2S_6$ freeze between 190 and 150 K into single off-center sites to form an ordered antipolar sublattice; the formation of this alternating up-and-down displacement array is accompanied by a loss of both the C translation and the center of inversion so that the RT $C2/c$ structure is described by the space group Pc at low temperatures [35]. This latter observation gave the first example of a structural transition in the $M^{I}M'^{III}P_2S_6$ phases and ruled out the occurrence of Cu_2S_6 entities as well as supported a thermal hopping interpretation of the RT copper disorder in these compounds [35].

It thus seems that the $CuM^{III}P_2S_6$ structure is capable of generating ordered copper sublattices. The temperature at which the ordering transition occurs and the nature of the ordered phase appear to vary with the trivalent half of the metal cation couple. An obvious way of further exploring this problem is the extension of this class of materials to other M(III) ions. In this article we report a single-crystal X-ray study of the RT structure of one such new compound, $CuInP_2S_6$.

2. Experimental details

The title material was prepared from a mixture of the elements in stoichiometric proportions and heated in evacuated silica tubes for two weeks at 600 °C. Air-stable yellow platelets embedded in a homogeneous powder bulk were thus obtained. Chemical analysis by means of an energy-dispersive-spectroscopy-equipped scanning electron microscope led to the expected stoichiometry within experimental accuracy. Traces of Cu_3PS_4 were detected in some preparations, but pure samples could also be successfully obtained. A magnetic susceptibility measurement was carried out in the 5–300 K range using a commercial superconducting quantum interference device magnetometer and showed the compound to be diamagnetic with $\chi_{dia} \approx -200\times10^{-6}$ emu mol^{-1}, close to the value calculated from Pascal's constants.

The crystal symmetry and cell parameters were initially estimated from classical rotating and Weissenberg analyses. The conditions limiting possible reflections corresponded to the $C2/c$ or Cc space groups, as observed for $CuCrP_2S_6$ [16]. The RT cell parameters were then least squares refined from powder data obtained using CuK L_3 radiation and an INEL CPS120 curved detector calibrated with $Na_2Ca_3Al_2F_{14}$ [37]. The complete indexing of the first 190 observed reflections with $\delta|2\theta|_{mean} = 0.011°$ yielded the monoclinic cell parameters reported in Table 1. The measured density is in very good agreement with the value calculated for this set of parameters and $Z=4$ (see Table 1).

Table 1
Crystallographic data for $CuInP_2S_6$ (data collected at 295(1) K)

Chemical formula	$CuInP_2S_6$
Formula weight	432.7 g
Color	Yellow
Space group	Cc (No. 9)
Lattice parameters	
a	6.0956(4) Å
b	10.5645(6) Å
c	13.6230(8) Å
β	107.101(3)°
V	838.5(1) Å^3
Z value	4
Measured density; calculated density	3.405 g cm^{-3}; 3.427 g cm^{-3}
Crystal size	0.09 mm×0.09 mm×0.02 mm
Radiation	MoK $L_{2,3}$ (λ=0.71073 Å)
Absorption coefficient μ	70.17 cm^{-1}
Recording angle range (θ)	1.5–35°
Number of unique reflections used in refinement	1987 ($I>3\sigma(I)$)
Number of refined parameters	96
Final R [a], R_w [b]	0.051, 0.056
Extinction coefficient	1.5×10^{-6}

[a] $R=\Sigma(|F_o|-|F_c|)/\Sigma|F_o|$.
[b] $R_w=(\Sigma w(|F_o|-|F_c|)^2/\Sigma wF_o^2)^{1/2}$; $w=1/\sigma^2(F_o)$.

To remove the ambiguity concerning the centrosymmetry or the non-centrosymmetry of the crystal structure an optical test was performed on a powder sample using an yttrium aluminum garnet laser and a $\lambda/2$ detection device. A second-harmonic generation signal was detected, implying non-centrosymmetry of the RT crystal structure. Structure refinements were then carried out within the acentric space group Cc.

Diffraction data from a small flat crystal approximately 0.09 mm×0.09 mm×0.02 mm in size were measured at RT on a CAD4-Kappa diffractometer (Enraf–Nonius) under standard recording conditions. The intensities of 3801 reflections from half of the reciprocal space were recorded with the systematic null reflections due to the C centering of the monoclinic cell omitted. After corrections for Lorentz, polarization and absorption effects (gaussian type) a set of 1987 independent reflections with $I>3\sigma(I)$ was obtained for structure refinements. Calculations and refinements were carried out using the MOLEN [38] and PROMETHEUS [39] program packages. Table 1 gathers some chemical and crystallographic data together with some data collection and refinement conditions.

3. Structure refinement

The indium position was first disclosed by a Patterson map and the P_2S_6 stacking revealed by Fourier and difference Fourier maps. After a few cycles, the In, P and S atomic positions and isotropic factors were refined to a reliability factor $R=0.182$.

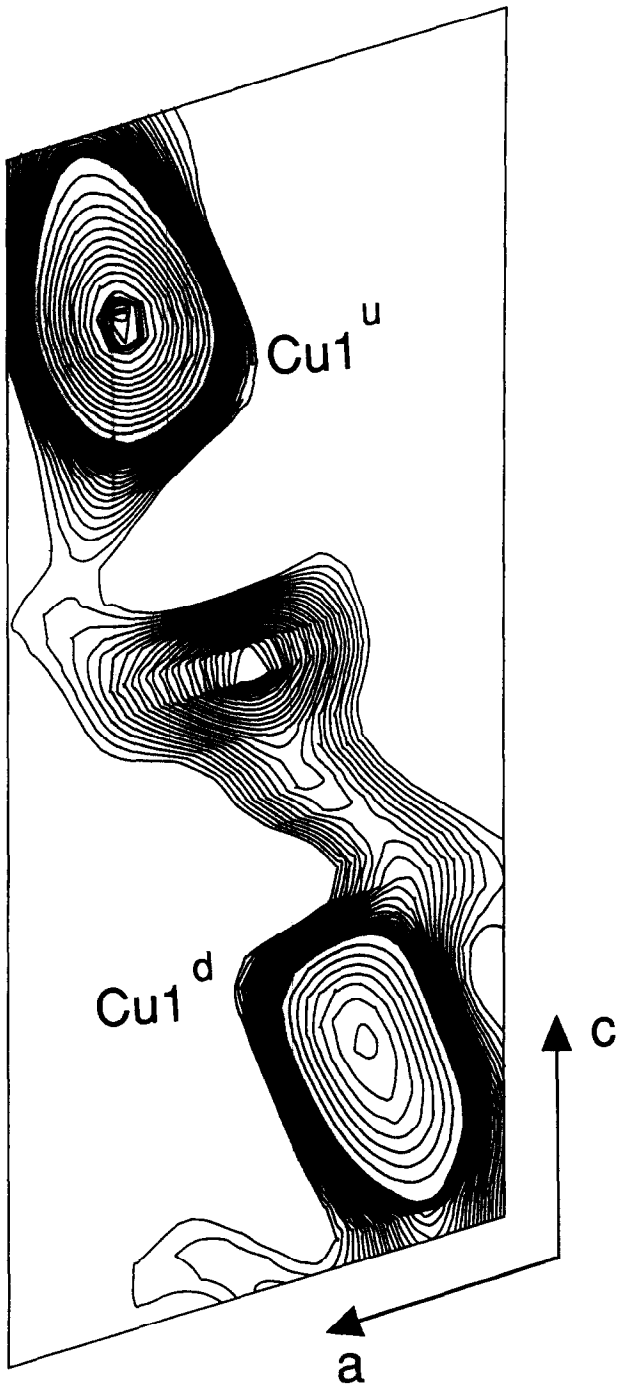

Fig. 1. A (010) section at $y=0.335$ of the difference Fourier map before the introduction of the two Cu(1)^u and Cu(1)^d copper positions in the structure refinement, showing the two inequivalent upper and lower maxima together with the very weak diffuse intensity located near the center. Contour lines from 0.0 to 44.7 e^- Å^{-3} in mean intervals of 2 e^- Å^{-3} are shown.

A new difference Fourier map was then calculated to locate the copper. This gave an electron density cloud located in a sulfur octahedron and elongated along the c^* axis with two maxima of unequal height close to the triangular faces and a diffuse density around the center (Fig. 1). Upon introducing two independent

Table 2
Positional and isotropic equivalent atomic displacement parameters for $CuInP_2S_6$ where the estimated standard deviations in the least significant figure are given in parentheses

Atom	x	y	z	B_{eq} [a] (Å^2)	τ [b]
Cu(1)^u	0.0957(3)	0.3355(2)	0.3869(2)	4.23(4)	0.875(4)
Cu(1)^d	−0.069(3)	0.335(2)	0.149(1)	3.7(3)	0.100(4)
In	0.000	0.00192(7)	0.250	1.634(9)	
P(1)	0.5686(3)	0.1690(3)	0.3491(2)	1.12(4)	
P(2)	0.4505(4)	0.1674(3)	0.1788(2)	1.36(4)	
S(1)	0.2808(4)	0.1512(2)	0.3950(2)	1.47(4)	
S(2)	0.2332(4)	0.1645(3)	0.8930(2)	1.49(4)	
S(3)	0.7845(4)	0.0177(2)	0.3950(2)	1.58(4)	
S(4)	0.7400(4)	0.1727(3)	0.1336(2)	1.82(4)	
S(5)	0.7555(4)	0.1747(3)	0.6404(2)	1.71(4)	
S(6)	0.2722(4)	−0.0057(3)	0.6379(2)	1.81(4)	

[a] Isotropic equivalent atomic displacement parameters defined as

$$B_{eq}=\frac{8\pi^2}{3}\sum_i\sum_j U_{ij}\,|\,\vec{a}_i^*\,\|\,\vec{a}_j^*\,|\,\vec{a}_i\cdot\vec{a}_j$$

[b] Site occupation ratios.

off-center positions Cu(1)^u and Cu(1)^d (u for up and d for down) with free site occupation ratios, the R factor dropped to 0.092, the site occupation ratios becoming 87% (Cu(1)^u) and 10% (Cu(1)^d). Refinement of the Cu(1)^u anisotropic atomic displacement parameters (ADP) $U(i,j)$ brought R down to 0.051. The low occupation ratio for Cu(1)^d precluded refining the displacement parameters beyond an isotropic ADP. The final difference Fourier map showed a smeared electronic density with a 1.25 e^- Å^{-3} maximum around the center of the copper octahedron as well as a lesser feature (1 e^- Å^{-3}) in the vdW gap. An attempt to refine with a central copper site led to a position shifted in the z^* direction and an occupancy ratio that tended towards zero. Since the vdW gap position was not in the original Fourier map and exhibited an electronic density weaker than that of the non-stable central site, it was likewise not considered as truly occupied. It should be noted that no significant decrease in the R factor could be achieved by refining with these latter two copper positions added to Cu(1)^u and Cu(1)^d. Therefore these positions were ruled out. An alternative description of the copper electronic distribution was sought by including some anharmonic terms of the ADPs (Gram–Charlier formalism [40]), particularly to model the central density better. However, none of the various expansions tried yielded improvements over the results of the harmonic split-atom model.

The final atomic coordinates with the equivalent isotropic ADPs, anisotropic ADPs, principal sulfur-to-cation distances and interatomic angles for $CuInP_2S_6$ are gathered in Tables 2, 3, 4 and 5 respectively. The sulfur–sulfur distances are given in Fig. 2.

Table 3
Anisotropic atomic displacement parameters $U(i,j)$ for $CuInP_2S_6$, where the estimated standard deviations in the least significant figure are given in parentheses. The form of the anisotropic displacement parameter is $\exp[-2\pi^2(h^2a^{*2}U(1,1)+k^2b^{*2}U(2,2)+l^2c^{*2}U(3,3)+2hka^*b^*U(1,2)+2hla^*c^*U(1,3)+2klb^*c^*U(2,3))]$. The low occupation ratio for Cu(1)[d] precluded refining the anisotropic parameters beyond an isotropic factor B_{iso} given in Table 2

Atom	U(1,1) (Å²)	U(2,2) (Å²)	U(3,3) (Å²)	U(1,2) (Å²)	U(1,3) (Å²)	U(2,3) (Å²)
Cu(1)[a]	0.0244(6)	0.0177(7)	0.126(1)	−0.0004(7)	0.0340(7)	0.001(1)
In	0.0180(2)	0.0188(2)	0.0261(2)	0.0003(4)	0.0077(2)	0.0007(4)
P(1)	0.0109(8)	0.0127(9)	0.0186(9)	0.0003(8)	0.0040(7)	0.000(1)
P(2)	0.0157(9)	0.018(1)	0.0187(9)	0.000(1)	0.0056(7)	0.001(1)
S(1)	0.0152(7)	0.019(1)	0.0240(9)	−0.0011(9)	0.0099(6)	−0.005(1)
S(2)	0.0158(8)	0.0159(9)	0.0243(9)	0.0044(9)	0.0048(7)	0.002(1)
S(3)	0.0201(8)	0.015(1)	0.0261(9)	−0.0030(8)	0.0091(7)	−0.0050(9)
S(4)	0.0177(8)	0.026(1)	0.028(1)	0.003(1)	0.0105(7)	0.004(1)
S(5)	0.0210(9)	0.018(1)	0.023(1)	0.003(1)	0.0009(8)	0.003(1)
S(6)	0.0246(8)	0.020(1)	0.0276(9)	0.009(1)	0.0125(7)	0.008(1)

Table 4
Principal interatomic distances in $CuInP_2S_6$ where the estimated standard deviations in the least significant figure are given in parentheses

Atom	Atom	Distance (Å)	Atom	Atom	Distance (Å)
Cu(1)[a]	S(1)	2.237(5)	P(2)	S(4)	2.034(4)
	S(2)	2.236(3)		S(5)	2.026(6)
	S(3)	2.228(5)		S(6)	2.014(7)
Cu(1)[d]	S(4)	2.05(3)	P(1)	P(2)	2.218(3)
	S(5)	2.02(2)	In	S(1)	2.708(4)
	S(6)	2.03(3)		S(2)	2.697(4)
P(1)	S(1)	2.037(4)		S(3)	2.680(3)
	S(2)	2.026(6)		S(4)	2.609(5)
	S(3)	2.048(5)		S(5)	2.573(5)
				S(6)	2.564(3)

Table 5
Principal interatomic angles in $CuInP_2S_6$ where the estimated standard deviations in the least significant figure are given in parentheses

	Angle (°)		Angle (°)
S(1)–In–S(2)	76.5(1)	S(3)–In–S(5)	98.5(1)
S(1)–In–S(3)	76.6(1)	S(4)–In–S(5)	90.2(1)
S(1)–In–S(4)	100.5(1)	S(4)–In–S(6)	90.6(2)
S(1)–In–S(6)	92.6(1)	S(5)–In–S(6)	91.8(1)
S(2)–In–S(3)	77.1(1)		
S(2)–In–S(5)	92.2(1)	S(1)–Cu(1)[a]–S(2)	119.2(2)
S(2)–In–S(6)	98.3(1)	S(1)–Cu(1)[a]–S(3)	120.2(1)
S(3)–In–S(4)	93.6(1)	S(2)–Cu(1)[a]–S(3)	120.0(2)

4. Structure description

The $CuInP_2S_6$ structure is similar to that of the other $Cu^IM^{III}P_2S_6$ phases (M(III) ≡ Cr or V); it is based on an ABC sulfur stacking and consists of a succession of $[SCu^I_{1/3}In^{III}_{1/3}(P_2)_{1/3}S]$ layers separated by a vdW gap, thus conferring a 2D character to the material (Fig. 3). A comparison of the three known $Cu^IM^{III}P_2S_6$ compounds is given in Table 6 which summarizes some of their RT structural characteristics. In all three cases, the octahedral voids defined by the sulfur framework are filled by the P–P pairs and the M cations such that a triangular sublattice is formed by each of these elements (Fig. 4). That the c parameter equals twice the interlayer distance in $CuInP_2S_6$ is due to an exchange of the P–P pair and copper locations from one layer to another. This contrasts with the case of $CuVP_2S_6$ but is reminiscent of that of $CuCrP_2S_6$ where a doubling is induced by an analogous P–P pair and Cr alternation

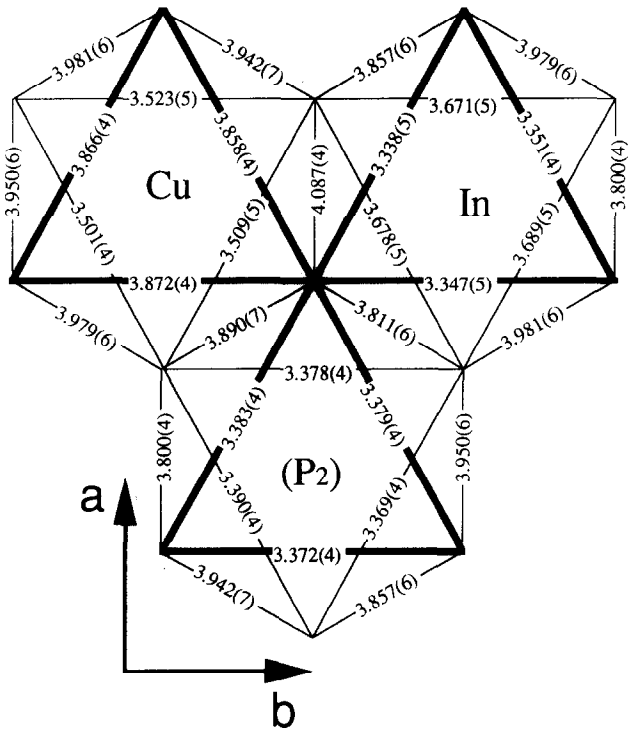

Fig. 2. Sulfur–sulfur distances (Å) in the different octahedra occurring in $CuInP_2S_6$.

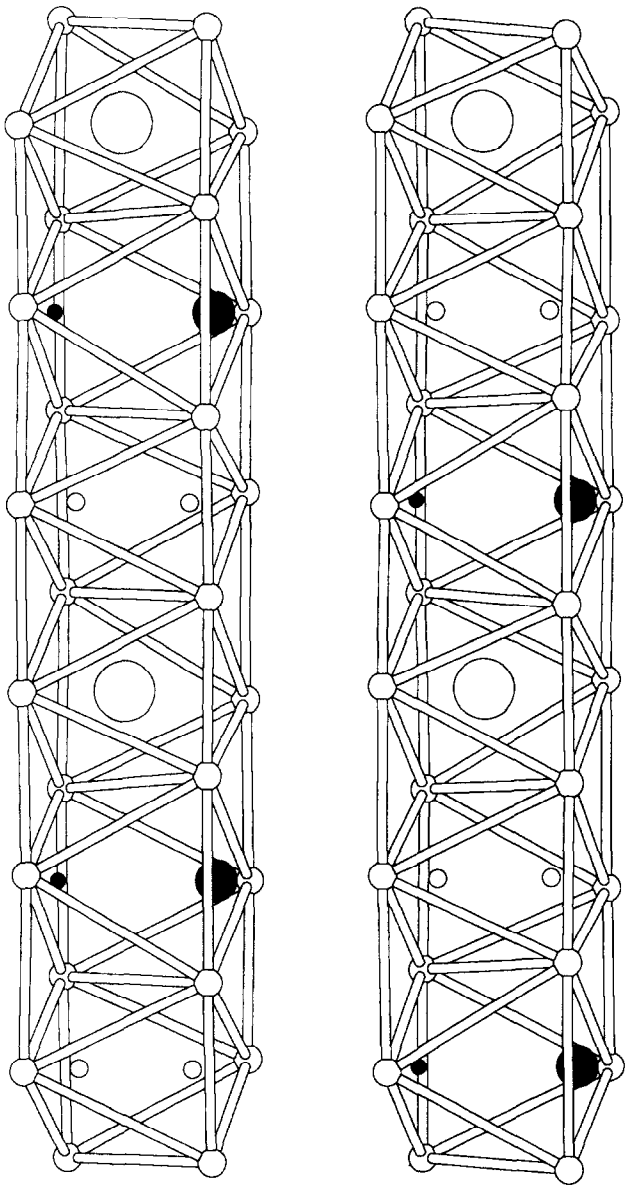

Fig. 3). Perspective view of two $[SCu^{I}_{1/3}In^{III}_{1/3}(P_2)_{1/3}S]$ layers (separated by the vdW gap) of $CuInP_2S_6$. Small, medium and large open circles represent P, S and In atoms, respectively. The copper positions are designated by full circles of two different sizes according to the occupation ratios.

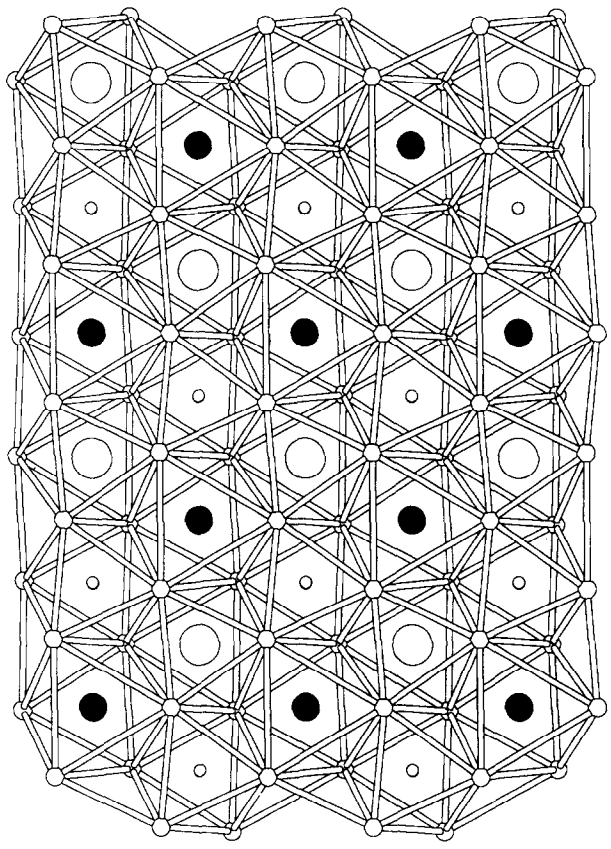

Fig. 4. View of the a–b plane showing the triangular arrangement of the metals and P–P groups in $CuInP_2S_6$. As in Fig. 3, small, medium and large open circles represent P, S and In atoms, respectively. The copper position are given by full circles.

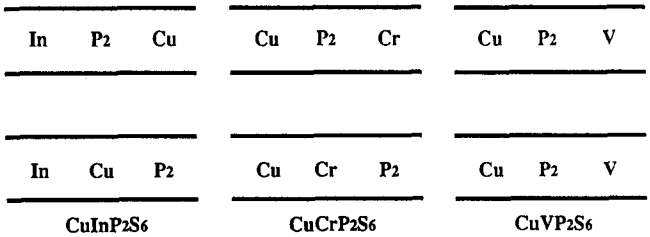

Fig. 5. A schematic representation of the arrangement of the cations and P–P pairs from one layer to another in the $Cu^{I}M^{III}P_2S_6$ phases (M(III) ≡ Cr, V or In) at RT.

Table 6
Room-temperature structural characteristics of $CuInP_2S_6$, $CuCrP_2S_6$ and $CuVP_2S_6$

	$CuInP_2S_6$ (this work)	$CuCrP_2S_6$ [16,45]	$CuVP_2S_6$ [21]
Space group	*Cc*	*C2/c*	*C2*
a (Å)	6.0956(4)	5.9217(5)	5.9462(6)
b (Å)	10.5645(6)	10.2592(8)	10.2990(10)
c (Å)	13.6230(8)	13.3721(10)	6.6870(6)
β (°)	107.101(3)	106.705(14)	107.247(9)
V (Å^3)	838.5(1)	778.1(2)	391.1(1)
Z value	4	4	2
V/Z (Å^3)	209.6	194.5	195.6

(see Fig. 5 for comparison). Anyhow, the *V/Z* ratio increases with increasing trivalent metal size if we consider that Cr(III) is smaller than V(III) (see Table 6).

The least-squares refinement using the split-atom model yielded two inequivalent sites per copper octahedron: one near the upper ($Cu(1)^u$) and the other near the lower ($Cu(1)^d$) sulfur triangle. This is quite different from the RT split-atom descriptions given for $CuCrP_2S_6$ [16] and $CuVP_2S_6$ [21] which assume four and six positions respectively per sulfur cage: two near the basal triangular faces (Cu(1)), two slightly shifted from the center (Cu(2)) and, in the latter compound, two tetrahedral sites in the vdW gap (Cu(3)). In these

two compounds, the members of each Cu(1), Cu(2) and Cu(3)-type pair are related by a twofold axis passing through the octahedron center, so that the number of independent crystallographic positions for copper is half the number of copper sites [16,21]. The nearly triangular, nearly central and tetrahedral positions are occupied with respective ratios of 0.53, 0.278 and 0.132 in $CuVP_2S_6$ [21], whereas the first two types of position are occupied with 0.66 and 0.34 ratios in $CuCrP_2S_6$ [16].

In $CuInP_2S_6$, almost 90% of the copper is found in the upper $Cu(1)^u$ position which is very near the octahedral triangular face as the S–$Cu(1)^u$–S angles indicate (Table 5). The $Cu(1)^u$–S distances vary from 2.228 to 2.237 Å (see Table 4), i.e. they are significantly longer than those found in $CuVP_2S_6$ and $CuCrP_2S_6$ at RT ($d_{Cu(1)-S(av)} = 2.128$ Å and 2.129 Å respectively [16,21]). These are, however, close to those observed in $CuCrP_2S_6$ at 64 K ($d_{Cu-S(av)} = 2.21$ Å) in which the copper atoms are frozen in either an upper or lower off-center position [35]. Correlatively, the average S–S distance ($d_{S-S(av)} = 3.865$ Å; see Fig. 2) within the upper triangular face in $CuInP_2S_6$ is longer than those observed in the Cr and V compounds at RT ($d_{S-S(av)} = 3.64$ Å and 3.75 Å respectively [16,21]) but compares well with that observed in $CuCrP_2S_6$ at 64 K ($d_{S-S(av)} = 3.83$ Å [35]). The longer $Cu(1)^u$–S distances is thus attributable to a swelling of the upper S triangle as in the said low temperature phase. The structure compensates for this expansion with a contraction of the upper triangle of the adjacent indium octahedra ($d_{S-S(av)} = 3.345$ Å; see Fig. 2) which suggests an off-centering of this cation towards the larger lower triangle ($d_{S-S(av)} = 3.679$ Å). The $U(i, j)$ values for $Cu(1)^u$ (see Table 3) are similar to those found in $CuCrP_2S_6$ [16] and $CuVP_2S_6$ [21] for copper positions near the basal sulfur triangles. Specifically, the predominant $U(3,3)$ values (0.126, 0.171 and 0.148 Å^2 for M ≡ In, Cr and V respectively) are characteristic of the strong anisotropy of the copper electron cloud in these three materials.

The remaining approximately 10% of the copper occupies the $Cu(1)^d$ position which is shifted down from the octahedral center. The lower S triangles are compressed ($d_{S-S(av)} = 3.551$ Å) and a mean $d_{Cu(1)^d-S} = 2.03$ Å, much smaller than found for $Cu(1)^u$ as well as for $CuVP_2S_6$ and $CuCrP_2S_6$, is calculated.

The average indium–sulfur distance ($d_{In-S(av)} = 2.638$ Å herein) is consistent with that found in $AgInP_2S_6$ ($d_{In-S(av)} = 2.646$ Å [19]) and with distances characteristic of an octahedral sulfur environment (2.630 Å) as tabulated by Tretyakov et al. [41]. However, two sets of indium–sulfur distances are found as shown in Table 4. One set of longer distances (2.708, 2.697 and 2.680 Å) corresponds to the sulfur atoms S(1), S(2) and S(3) forming the upper triangle of the In octahedron, as well as that of the adjacent $Cu(1)^u$. The other set of shorter lengths (2.609, 2.573 and 2.564 Å) is associated with the $Cu(1)^d$-bonded sulfur atoms S(4), S(5) and S(6) which form the larger lower triangle of the InS_6 unit (Fig. 2). Two sets of sulfur–indium–sulfur angles are also inferred from Table 5 (compare S(1)–In–S(2), S(1)–In–S(3), S(2)–In–S(3) angles with S(4)–In–S(5), S(4)–In–S(6), S(5)–In–S(6) angles). It may thus be concluded that the In ion indeed occupies an off-center position within its octahedron; it is shifted by about 0.2 Å approximately along the perpendicular to the slab towards the lower S triangle.

The average phosphorus–sulfur bond length ($d_{P-S(av)} = 2.031$ Å) agrees with the values calculated in the MPS_3 phases ($d_{P-S(av)} = 2.028$–2.034 Å [42–44]) and other $M^IM'^{III}P_2S_6$ compounds ($d_{P-S(av)} = 2.028$–2.034 Å [16–21]). On the contrary, the phosphorus–phosphorus distance ($d_{P-P} = 2.217$ Å) is slightly longer than the value calculated for the other $Cu^IM^{III}P_2S_6$ ($d_{P-P} = 2.165$ Å and 2.168 Å for M ≡ Cr or V respectively [16–21]) and for most of the MPS_3 (M ≡ Mn, Fe, Co, Ni or Zn; $d_{P-P} = 2{,}147$–2.188 Å [42–43]), except for M(II) ≡ Cd(II) ($d_{P-P} = 2.222$ Å [42,44]) which is isoelectronic with In(III).

5. Discussion

The RT distribution of copper atoms within its sulfur octahedron in $CuInP_2S_6$ may be interpreted in two different ways. The first would assume that 90% of the copper octahedra exclusively contain fully occupied $Cu(1)^u$ positions while 10% have only the $Cu(1)^d$ filled; the electronic density in Fig. 1 then results from a spatial average over all such statically filled octahedra. Alternatively, the structure could contain octahedra with the $Cu(1)^u$ and $Cu(1)^d$ positions being occupied 90% and 10% respectively of the time; the distribution then corresponds to superposed "snapshots" of a copper ion hopping between the two positions.

As mentioned in the introduction, neutron powder diffraction experiments on $CuVP_2S_6$ and $CuCrP_2S_6$ [34,35] have shown that cooling leads to the emptying of the nearly central Cu(2) positions; the implication is that occupation of the triangular Cu(1) site is then favored because the thermal energy available for hopping diminishes at low T. Quite apart from these results, a calculation of the RT effective one-particle potential for Cu in $CuCrP_2S_6$ based on the structural parameters of [16] revealed a simple double-well shape [45]. Thus the central flat maximum of the RT copper electronic density does not correspond to an equilibrium position but is rather indicative of a non-zero probability that the copper ion passes through the center as it hops from one well to the other [45]. Also, the non-existence of a static Cu octahedral coordination and the presence of triangular and tetrahedral energy minima in the $Cu^IM^{III}P_2S_6$ materials are consistent with stereochemical

considerations [17,21,46] and may be related to the possible occurrence of a second-order Jahn–Teller effect [20]. Furthermore, the high quadrupolar polarizability of copper(I) would favor the ionic mobility [21].

We hence believe that the RT X-ray picture of the copper distribution in $CuInP_2S_6$ represents a temporal average of the thermal hopping between the two $Cu(1)^u$ and $Cu(1)^d$ positions. Within this model, the 0.9/0.1 occupation ratios reflect different depths for two wells and signal the probable existence of a completely polar copper sublattice at temperature below ambient. The much weaker central electronic density, compared with that in $CuCrP_2S_6$ and $CuVP_2S_6$ at RT, supports this latter assumption.

The indium downward displacement is obviously related to the features of the adjacent copper distribution. It may also be favored by the closed-shell electronic configuration of In(III) for which no crystal field stabilization is expected. In the MPS_3 series, it has been pointed out that the equivalent ADP B_{eq} of the M(II) ions are strongly correlated with their ligand field stabilization [42]. We note that a similar correlation may exist in the $Cu^IM^{III}P_2S_6$ phases since B_{eq} decreases with M(III) ≡ In(III), V(III) and Cr(III) ($B_{eq} = 1.6$ Å^2, 1.2 Å^2 and 0.6 Å^2 respectively [16,21]).

The particular features of both the copper distribution and the In off-centering in $CuInP_2S_6$ are related to the known flexibility of the 2D P_2S_6 stacking. In the MPS_3 series, the P–P distance varies to accommodate the metal size, while the PS_3 group behaves like a rather rigid entity [42]. In the chain-containing $AgCrP_2S_6$ and $AgVP_2S_6$, however, the easy elongation of the P–P bond cannot compensate for the large metallic cation size difference which induces a significant dispersion of the P–S distances (about 0.07 Å) [17,18]. Matching of the P_2-containing octahedron size with those of the metals is thus ensured by a length modulation of the edge shared by the octahedra [18].

In $CuInP_2S_6$, the structure ostensibly accommodates the relatively large indium cation by increasing the P–P bond length but the dispersion of the P–S bond distances is rather small (about 0.03 Å, see Table 4). Since the PS_3 units strongly oppose any contraction or expansion [27], the swelling or squeezing in the basal triangles of Cu and In octahedra imply a concerted rotation of the upper and lower PS_3 units, leading to a twisting of the P_2S_6 units which becomes apparent with a close look at Fig. 4. Those rotations generate a widening of all the $Cu(1)^u$ potential sites, whether occupied or not, the shrinking of an empty triangle being unstable against the concerted rotations. The situation is totally different at the $Cu(1)^d$ lower site. The concomitant rotations of the triangles would lead to a contraction of all the potential $Cu(1)^d$ basal triangles, whatever the occupation. However, the presence of copper atoms in about 10% of those sites creates local frustrations reflected in the equivalent ADPs of the lower triangle S atoms which are larger than those of the upper triangle (1.82, 1.71 and 1.81 Å^2 against 1.47, 1.49 and 1.58 Å^2, see Table 2).

Concerted rotations of PS_3 entities are also observed in the triangular compounds $CuCrP_2S_6$ [16], $CuVP_2S_6$ [21] and $Ag_2MnP_2S_6$ [27,36]. On the contrary, such twisting motions cannot occur in the chain-containing $AgCrP_2S_6$ and $AgVP_2S_6$ for simple geometric reasons.

6. Conclusions

In this paper we have reported a single-crystal analysis of the RT structure of a new member of the two-dimensional $CuM^{III}P_2S_6$ family, $CuInP_2S_6$. While its overall structure resembles those of $CuVP_2S_6$ and $CuCrP_2S_6$, it distinguishes itself via the predominant occupation of an upper triangular Cu site and the off-centering of the In atom, both of which signal the probable formation of a completely polar copper sublattice at lower temperatures in agreement with a thermal hopping process of the copper atoms. Obviously, these results call for additional temperature-dependent studies of all three materials, including diffraction, vibrational spectroscopies and physical measurements, specifically to define better and thus to understand the differences between these compounds.

The study of the recently reported analogous compounds $CuM^{III}P_2Se_6$ (M ≡ Cr, In or Al) [47,48] should likewise be informative. As in $CuM^{III}P_2S_6$, the structures of these phases are based on a succession of $[SeCu^I_{1/3}M^{III}_{1/3}(P_2)_{1/3}Se]$ layers within which the P_2 pairs and metal cations occupy the selenium octahedra. Copper distributions similar to those found in the corresponding thiophosphates may thus be expected. However, the RT powder X-ray analyses of these structures have used only one central position for copper with a high isotropic thermal factor [47,48]; furthermore, the proposed arrangement of the metals within a slab in $CuCrP_2Se_6$ contradicts recent magnetic susceptibility measurements [49]. The RT structures of $CuM^{III}P_2Se_6$ are currently being reinvestigated using powder neutron diffraction to shed more light on the physicochemical origins of the interesting copper behaviour in the extended family of $CuM^{III}P_2X_6$ (X ≡ S or Se) compounds.

Acknowledgements

We thank L. Cot and his colleagues for performing the second harmonic generation test and acknowledge R. Brec, P. Colombet and A. Leblanc for useful discussions. V.M. thanks E. Durand, A. Van Der Lee and

F. Boucher for their help in using the refinement programs.

Supplementary materials available

Tables of complete crystallographic data and observed and calculated structure factors are available from the authors.

References

[1] R. Brec, *Solid State Ionics, 22* (1986) 3, and references cited therein.
[2] E.J.K.B. Banda, *J. Phys. C, 19* (1986) 7329.
[3] K. Okuda, K. Kurosawa, S. Saito, M. Honda, Z. Yu and M. Date, *J. Phys. Soc. Jpn., 55* (1986) 4456.
[4] M. Balkanski, M. Jouanne, G. Ouvrard and M. Scagliotti, *J. Phys. C., 20* (1987) 4397.
[5] M. Barj, G. Lucazeau, G. Ouvrard and R. Brec, *Eur. J. Solid State Inorg. Chem., 25* (1988) 449.
[6] N. Nagasundaram and A.H. Francis, *J. Phys. Chem. Solids, 50* (1989) 163.
[7] S. Torre and J. Ziolo, *Phys. Rev. B, 39* (1989) 8915.
[8] N. Kurita and K. Nakao, *J. Phys. Soc. Jpn., 58* (1989) 232, 610.
[9] V. Grasso, F. Ferri, S. Patane and L. Silipigni, *Phys. Rev. B, 42* (1990) 1690.
[10] G. Ouvrard and R. Brec, *Eur. J. Solid Inorg. Chem., 27* (1990) 477.
[11] R. Clement, L. Lomas and J.P. Audiere, *Chem. Mater., 2* (1990) 641.
[12] V. Grasso, F. Neri, L. Silipigni and M. Piacentini, *Nuovo Cim. D, 13* (1991) 633.
[13] J.A. Read, C. Chick and A.H. Francis, *J. Phys. Chem., 96* (1992) 2010.
[14] P.A. Joy and S. Vasudevan, *Phys. Rev. B, 46* (1992) 5425.
[15] P.A. Joy and S. Vasudevan, *Chem. Mater, 5* (1993) 1182.
[16] P. Colombet, A. Leblanc, M. Danot and J. Rouxel, *J. Solid State Chem., 41* (1982) 174.
[17] P. Colombet, A. Leblanc, M. Danot and J. Rouxel, *Nouv. J. Chim., 7* (1983) 333.
[18] S. Lee, P. Colombet, G. Ouvrard and R. Brec, *Mater. Res. Bull., 21* (1986) 917.
[19] Z. Ouili, A. Leblanc and P. Colombet, *J. Solid State Chem., 66* (1987) 86.
[20] S. Lee, P. Colombet, G. Ouvrard and R. Brec, *Inorg. Chem., 27* (1988) 1291.
[21] E. Durand, G. Ouvrard, M. Evain and R. Brec, *Inorg. Chem., 29* (1990) 4916.
[22] Y. Mathey, R. Clement, J.P. Audiere, O. Poizat and C. Sourisseau, *Solid State Ionics, 9–10* (1983) 459.
[23] Y. Mathey, A. Michalowicz, P. Toffoli and G. Vlaic, *Inorg. Chem., 23* (1984) 897.
[24] O. Poizat and C. Sourisseau, *J. Solid State Chem., 59* (1985) 371.
[25] O. Poizat, F. Sourisseau and Y. Mathey, *J. Solid State Chem., 72* (1988) 272.
[26] O. Poizat, C. Fillaux and Y. Mathey, *J. Solid State Chem., 72* (1988) 283.
[27] M. Evain, F. Boucher, R. Brec and Y. Mathey, *J. Solid State Chem., 90* (1991) 8.
[28] F. Boucher, M. Evain and R. Brec, *Eur. J. Solid State Inorg. Chem., 28* (1991) 383.
[29] S. Lee, *J. Am. Chem. Soc., 110* (1988) 8000.
[30] H. Mutka, C. Payen, P. Molinie, J.L. Soubeyroux, P. Colombet and A.D. Taylor, *Phys. Rev. Lett., 67* (1991) 497.
[31] H. Mutka, C. Payen and P. Molinié, *Europhys. Lett., 21* (1993) 623.
[32] Y. Mathey, H. Mercier, A. Michalowicz and A. Leblanc, *J. Phys. Chem. Solids, 46* (1985) 1025.
[33] C. Payen, P. McMillan and P. Colombet, *Eur. J. Solid State Inorg. Chem., 27* (1990) 881.
[34] G.L. Burr, E. Durand, M. Evain and R. Brec, *J. Solid State Chem., 103* (1993) 514.
[35] V. Maisonneuve, V.B. Cajipe and C. Payen, *Chem. Mater., 5* (1993) 758.
[36] A. van der Lee, F. Boucher, M. Evain and R. Brec, *Z. Kristallogr., 203* (1993) 247.
[37] M. Evain, P. Deniard, A. Jouanneaux and R. Brec, *J. Appl. Crystallogr., 26* (1993) 563.
[38] C. Kay Fair, MOLEN: Structure Determination Package, Enraf–Nonius, 1982.
[39] U.H. Zucker, E. Parenthaler, W.F. Kuhs, R. Bachmann and H. Schulz, *J. Appl. Crystallogr., 16* (1983) 358.
[40] U.H. Zucker and H. Schulz, *Acta Crystallogr., Sect. A, 38* (1983) 563.
[41] Y.D. Tretyakov, I.V. Gordeev and Y.A. Kesler, *J. Solid State Chem., 20* (1977) 345.
[42] R. Brec, G. Ouvrard and J. Rouxel, *Mater. Res. Bull., 20* (1985) 1257.
[43] E. Prouzet, G. Ouvrard and R. Brec, *Mater. Res. Bull., 21* (1986) 195, 643.
[44] F. Boucher, M. Evain and R. Brec, *J. Alloys Comp., 215* (1994) 63.
[45] V. Maisonneuve, C. Payen and V.B. Cajipe, to be published.
[46] A.F. Wells, *Structural Inorganic Chemistry,* Oxford University Press, Oxford, 1984, p. 1103.
[47] R. Pfeiff and R. Kniep, *J. Alloys Comp., 186* (1992) 111.
[48] R. Pfeiff and R. Kniep, *Z. Naturforsch., 48b* (1993) 1270.
[49] V.B. Cajipe, J.E. Fischer, V.M. Maisonneuve and C. Payen, to be published.